Superheating, Melting, and Annealing of Copper Surfaces

H. Häkkinen* and Uzi Landman
School of Physics, Georgia Institute of Technology, Atlanta, Georgia 30332
(Received 8 March 1993)

Dynamics of superheating, melting, and annealing processes at Cu(111) and Cu(110) surfaces, induced by laser-pulse irradiation, are investigated using molecular dynamics simulations, incorporating energy transfer from the electronic to the ionic degrees of freedom. Superheating occurs at Cu(111) for conditions that lead to melting of the Cu(110) surface. Highly damaged Cu(111) surfaces structurally anneal under the influence of a superheating pulse.

PACS numbers: 61.80.Ba, 61.72.Cc, 68.35.Ja, 68.35.Rh

Methods of processing of materials surfaces via laser irradiation are of fundamental as well as technological and economic significance, since various physical and chemical surface properties (such as optical and electrical characteristics, corrosion resistance, composition, morphology, and structure) can be influenced and/or modified using such methods in a controlled and spatially selective manner [1,2]. Furthermore, with the use of short laser pulses, detailed time-resolved experimental investigations of electron-phonon energy transfer mechanisms and relaxation times [3], and of the thermal and structural evolution of metal surfaces (disordering, melting [4(a)], and most recently superheating of the Pb(111) surface [4(b)], have been performed. In these experiments it was found, using time-resolved reflection high-energy electron diffraction (RHEED), that during and following a laser pulse irradiation the surface superheated up to 120 K above the bulk melting temperature (temperatures were determined from Debye-Waller analysis of the RHEED intensities) while maintaining crystalline order.

Commonly laser processing of solid surfaces is discussed in the context of laser heating, melting, and subsequent solidification (or recrystallization) of the surface region of the sample [1,2]. Although the phenomenon of surface melting was proposed over a century ago [5] it is only during the past decade that controlled experimental observations and theoretical studies have been made [6,7] of surface disordering, roughening, melting, and premelting (that is formation of a quasiliquid surface region for $T < T_m^b$, where T_m^b is the bulk melting temperature of the material). Both experimental [4,6] and theoretical [7,8] studies have shown that premelting can occur for the (110) surfaces of certain fcc metals [e.g., Pb(110) [4(a),6], Al(110) [7(a)], and Cu(110) [7(b),8], while Ni(110) [7(c)], as well as the close-packed (111) surfaces of fcc metals do not premelt [6,7(b)]], with the premelting propensity determined by the sign and magnitude of the interfacial free-energy difference $\Delta\gamma$ between the ordered solid surface and the surface wetted by its melt ($\Delta\gamma > 0$ corresponds to premelting tendency, thus precluding superheating for surfaces with $\Delta\gamma > 0$). Furthermore, molecular dynamics (MD) simulations [7,8] show that the nucleation mechanisms of the premelting process involve generation of vacancy-adlayer atom pairs, with the energy required for such processes significantly higher at close-packed fcc metal surfaces than at the (110) surface.

We report on molecular dynamics simulations of laser irradiation of copper surfaces which differ from continuum treatments of such phenomena [1] and previous simulations [2] by explicitly including the temporal laser excitation of the electrons and their coupling to the microscopic dynamics of the nuclear degrees of freedom which are modeled using realistic interactions. Our simulations demonstrate that under irradiation conditions for which the Cu(110), as well as Cu(100), surfaces undergo melting, superheating of perfect as well as damaged Cu(111) occurs, in correspondence with recent experiments [4(b),4(c)] on Pb(111). Moreover, under the same conditions, a damaged Cu(111) surface (containing initially a large vacancy cluster and an adlayer island) superheats and anneals, restoring perfect crystalline order, via a nondiffusional mechanism involving local incorporation (embedding) of adlayer atoms and subsequent cooperative displacements of the host surface layer atoms to fill the vacancy region. This finding is of particular relevance in light of the experimental observations [4(b)], where the sample surfaces are most likely to contain, even under equilibrium conditions, a certain fraction of spontaneously generated defects which could serve as nucleation centers for melting, and is related to the energetics of the (111) surface.

To simulate the dynamics of copper surfaces irradiated by a laser pulse we developed a MD method where the laser pulse deposits energy into the electronic subsystem, modeled as a uniform fluid, which couples locally to the ionic degrees of freedom whose dynamics is governed by many-body embedded-atom (EAM) potentials [9]. In a continuum model of the system (electronic and ionic) the time evolution of the electronic and lattice temperatures [$T_e(z,t)$ and $T_l(z,t)$] are described by two coupled nonlinear differential equations [10] (in conjunction with appropriate boundary conditions)

$$C_e(T_e)\frac{\partial T_e}{\partial t} = \kappa_e \frac{\partial^2 T_e}{\partial z^2} - G(T_e - T_l) + P(z,t)\,, \tag{1}$$

$$C_l(T_l)\frac{\partial T_l}{\partial t} = \kappa_l \frac{\partial^2 T_l}{\partial z^2} + G(T_e - T_l)\,, \tag{2}$$

where the characteristics of the laser pulse are given by

$$P(z,t)=I_0(1-R)ae^{-az}f(t-t_0)\,, \tag{3}$$

with a peak intensity I_0, an absorption coefficient α, a reflectivity R, and a Gaussian temporal shape profile $f(t-t_0)=\exp[-(t-t_0)^2/2\sigma^2]$, with the FWHM given by 2σ. In the above equations C_e,κ_e and C_l,κ_l are the heat capacities and thermal conductivities for the electronic and lattice subsystems, respectively, G is the electron-phonon coupling constant, and z is the direction normal to the surface.

To explore the microscopic dynamics of a surface exposed to laser-pulse irradiation we modify the above continuum formulation in conjunction with a classical MD simulation of the ionic dynamics. The system is divided in the z direction into two regions: a dynamic region (D) $0<z\le z_d$ (with the origin taken at the topmost crystalline layer) and a continuum region (C) for $z_d<z\le z_b$, where z_b is a position deep in the material. The ionic system in region D is set up in the desired crystallographic structure (with n_d dynamic layers, positioned on top of n_s static layers) in a calculational cell which is periodically replicated in the two directions parallel to the surface, and the equations of motion for the ions, interacting via EAM potentials, are integrated in this region (except for the bottom static substrate) using the fifth-order Gear predictor correlator algorithm [11] with a time step $\Delta t=5.1$ fs. In our simulations we use for the (110) surface $n_d=60$, $n_s=4$, and for the (111) surface $n_d=51$, $n_s=3$ [this corresponds to 88 and 100 atoms per layer, for the (110) and (111) systems, respectively, and the thickness of region D is ~ 100 Å].

The energy exchange between the electron fluid subsystem and the dynamic ions is implemented by introducing an additional term into the ionic equations of motion

$$M\frac{d^2\mathbf{R}_i}{dt^2}=-\nabla_{\mathbf{R}_i}E_{\mathrm{EAM}}(\{\mathbf{R}_i\})-\mu M\frac{d\mathbf{R}_i}{dt}\,, \tag{4}$$

where M and $\mathbf{R}_i$ are the mass and position vector of ion i. The first term on the right is the EAM force on the ith ion, and the coupling coefficient in the energy exchange term is given by [12(a)]

$$\mu=\mu(z,t)=(G/C_l)[\langle T_l(z,t)\rangle-T_e(z,t)]/\langle T_l(z,t)\rangle\,.$$

The electronic temperature $T_e(z,t)$ over the whole region $z\le z_b$ is obtained via solution of Eq. (1) between successive MD steps [using a Runge-Kutta-type second-order method [11], with a time-step $0.8(\delta z)^2/2D_e$, where $D_e=\kappa_e/C_e$ is the thermal diffusivity of the electrons, and δz corresponds to a length equal to 3 interlayer distances]. To get the lattice temperature profile $T_l(z,t)$, Eq. (2) (with the first term neglected) is solved for the region $z_d\le z\le z_b$. For the dynamic region $0<z<z_d$, $T_l=\langle T_l(z,t)\rangle$ is obtained from the particle kinetic energies by averaging the simulation trajectories over 25 Δt intervals in regions of thickness δz. The boundary conditions used in solving these equations are $T_e(z_b,t)=T_l(z_b,t)=T_b$ ($z_b=5000$ Å and $T_b=1100$ K), $dT_e(0,t)/dz=0$, and $dT_e(z_b,t)/dz=dT_l(z_b,t)/dz=0$. The material and pulse parameters which we use are

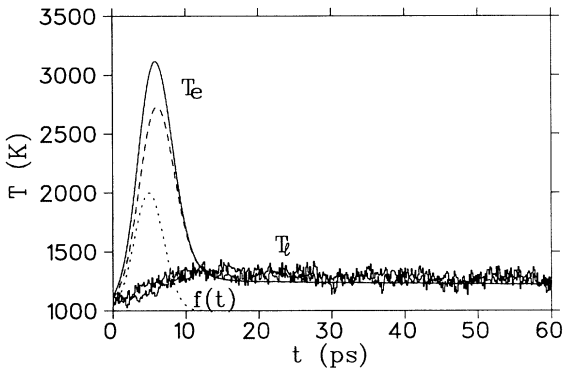

FIG. 1. Electronic temperature (T_e) at the surface region, consisting of the topmost two layers (solid), and deep in the dynamic region, near the static substrate (dashed), and the corresponding lattice (ionic) temperatures (T_l) obtained in a simulation using a superheating pulse $I_0=5\times10^9$ W/cm^2, starting from a Cu(111) surface equilibrated at 1100 K. Also shown is the temporal shape of the laser pulse (dotted line). Temperature and time in units of K and ps.

$C_e=96.6T_e$ J/m^{3}K [13(a)], $C_l=3.5\times10^6$ J/m^{3}K [13(a)], $\kappa_e=166$ W/mK [12(b),13(a)], $G=1\times10^{17}$ W/m^{3}K [3], $R=0.8$, and $\alpha=5\times10^8$ m^{-1} [13(b)].

Typical records of the electronic and lattice temperatures in our simulations are shown in Fig. 1 where we exhibit results obtained for a laser pulse, with $I_0=5\times10^9$ W/cm^2 (leading to superheating of the surface, see below), irradiating a Cu(111) surface, equilibrated initially at 1100 K. We observe significant heating of the electronic subsystem near the surface, as well as in a deeper region (though to a somewhat lower temperature, achieving a peak value slightly after the surface region), and a transfer of energy to the ionic degrees of freedom, whose temperature comes close (slightly above) to that of

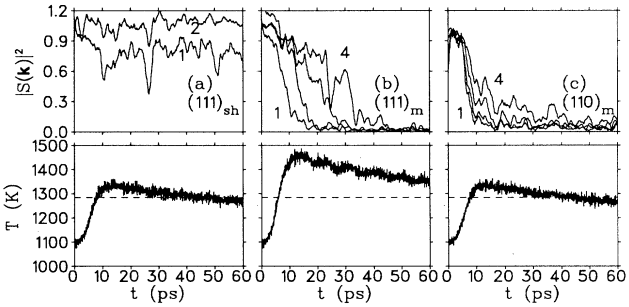

FIG. 2. Temporal evolution of the structure factor $|S(\mathbf{k})|^2$, for $\mathbf{k}=4\sqrt{2}\pi/a\sqrt{3}(0,1)$ for Cu(111) and $\mathbf{k}=2\pi/a(1,0)$ for Cu(110) and temperature of the whole dynamic system for laser irradiation MD simulations of (a) superheating of the Cu(111) surface; (b) melting of the Cu(111) surface; (c) melting of the Cu(110) surface. In the $|S(\mathbf{k})|^2$ plots the structure factors for individual layers are denoted by layer numbers, with the topmost surface layer $l=1$. The calculated bulk melting temperature ($T_m^b=1284$ K) is denoted by a dashed line in the temperature plots. $|S(\mathbf{k})|^2$ normalized to its value at the initial temperature $T=1100$ K. T in K and time in ps.

the electron fluid shortly after the termination of the laser pulse, equilibrating to T_e at longer times [14].

The temporal and spatial evolution of order and energetics for Cu(111) and Cu(110) are given in Figs. 2 and 3. Comparison of the order parameters for the (111) and (110) surfaces [Figs. 2(a) and 2(c), respectively], irradiated by the same laser pulse ($I_0 = 5 \times 10^9$ W/cm^2) shows that while the (110) surface [as well as the (100) surface, not shown] underwent melting induced by the laser heating, crystalline order is maintained at the (111) surface which remains superheated for ~ 40 ps, with the lattice temperature rising as much as 40 K over the calculated bulk melting point ($T_m^b = 1284$ K [7]). We further observe that irradiation by a higher-intensity pulse ($I_0 = 8 \times 10^9$ W/cm^2) does result in melting of the (111) surface [see Fig. 2(b)]. It is interesting to note that the disordering and melting of Cu(110) occurs simultaneously for a broader surface region [Fig. 2(c)], compared to the layer-by-layer process at the Cu(111) surface [Fig. 2(b)].

Further details pertaining to the structure of the laser irradiated surfaces are evident from the layer radial pair distributions $g_{\parallel}(r)$, shown in Fig. 3(c), where it is observed that long-range crystalline order is preserved at the superheated Cu(111)$_{SH}$ surface, whereas the $g(r)$ functions for the melted $(111)_m$ and $(110)_m$ surfaces are very similar, exhibiting characteristics reflecting the liquid nature of these surfaces. In this context we add that the calculated diffusion constants for these surfaces also reflect their liquid nature, while those corresponding to the superheated (111) surface are typical to a hot crystalline solid surface.

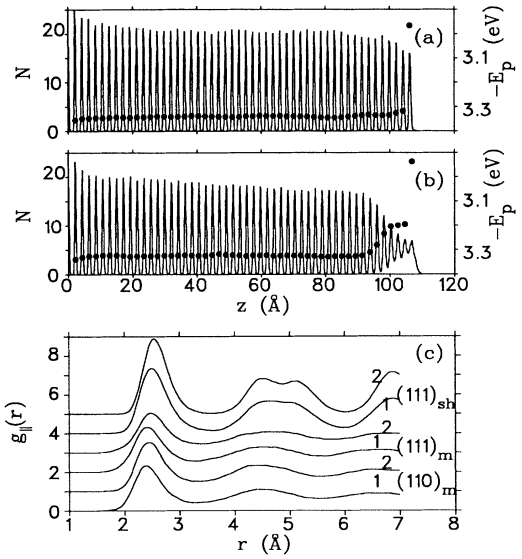

FIG. 3. (a),(b) Profiles of the number of particles N and potential energies (solid dots, right scale), versus z (the direction normal to the surface, with the origin taken at the first dynamic layer deep in the substrate) for superheated Cu(111) [in (a)] and melted Cu(111) [in (b)]. (c) Two-dimensional pair-distribution functions in individual layers (1 and 2 correspond to the topmost surface layer and the layer below it) of superheated and melted Cu(111) surfaces and a melted Cu(110) surface. Note the crystalline structure in the superheated surface, (111)$_{SH}$. Distance in the layer in Å.

The energetics of the superheated and melted Cu(111) surfaces shown in Figs. 3(a) and 3(b) portrays an increase in the potential energy of the Cu(111) surface irradiated by the higher intensity pulse [Fig. 3(b)]. Indeed, the increase in E_p is ~ 0.123 eV/atom, in agreement with the calculated [7] heat of melting of copper ($\Delta H_m = 0.125$ eV/atom, compared to the measured value of 0.136 eV/atom).

Having observed superheating of a perfect (111) surface it is instructive, for experimental as well as theoretical considerations, to inquire about the possible influence of defects on the ability to sustain a superheated state of a solid surface. Since surface melting has been observed to be initiated by generation of surface vacancies, we have performed simulations of laser irradiation of defective surfaces. Surprisingly, we observed superheating of Cu(111) surfaces even for highly defective surfaces (e.g., imperfect surfaces with up to 10% preexisting vacancies, either randomly distributed, or in a vacancy cluster). Moreover, laser irradiation of a Cu(111) surface which was equilibrated with a preexisting vacancy cluster (VC) and an adlayer island [see Fig. 4(a)], resulted in superheating coupled with annealing of the surface structure [see Fig. 4(b)]. The annealing process occurred via a nondiffusional mechanism. Rather, we observed local embedding (settling) of the adatoms into the underlying topmost surface layer inducing cooperative displacements in that layer and the layer below, resulting in contraction and eventual filling of the vacancy cluster [see Fig. 4(b)]. Interestingly, such a nondiffusional settling mechanism

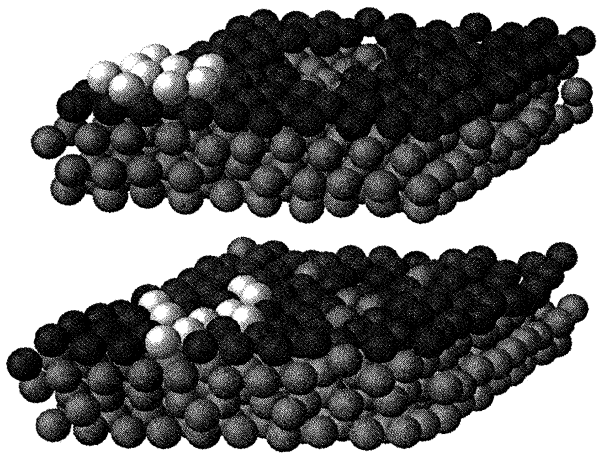

FIG. 4. Atomic configuration of a Cu(111) surface containing a vacancy cluster and an adlayer island (brightest atoms) prior to irradiation (top), and a configuration recorded 20 ps after the termination of a superheating laser pulse (bottom). Dark and grey spheres correspond to atoms in the topmost surface layer and in the layers below it. Note that in the annealed surface the atoms originating at the adlayer island did not migrate to fill the vacancy cluster.

was observed by us recently in the context of studies of stability and spreading mechanisms of metallic nanostructures supported on metal substrates [15].

The remarkable stability of Cu(111) [and the (111) surfaces of other fcc metals] against melting correlates with the high energy for formation of vacancy-adatom pairs (E_{vaf}) at the surface. An adequate estimate of E_{vaf} may be obtained by considering the change in coordination Δ_c of an atom when it is moved from its original position in the surface to the adlayer (i.e., the net number of "broken bonds"). The relative stability of Cu(111) as compared to the Cu(110) surface is reflected in the values $\Delta_c(111)=9-3=6$ and $\Delta_c(110)=7-5=2$, which together with $E_{vaf}(110)=0.4$ eV [7] yield a lower-bound estimate of $E_{vaf}(111)=1.2$ eV. [We remark that in a bond-breaking model the cohesive energy of a given atom varies linearly with coordination number (C). The many-atom interactions in EAM models result in a nonlinear dependence of $E(C)$ which effectively increases the change in energy when going to low C [16].] A similar argument applied to the (111) surface containing a VC shows that the energy cost for formation of a vacancy-adatom pair from the periphery of the VC is $(2-2.5)E_{vaf}(110)$ for the concave edge of the VC, and is larger than $E_{vaf}(110)$ even for the convex edge of the adatom island (see Fig. 4). Consequently the stability of such clustered defects on the (111) surface may be attributed to a relatively high "line tension" which prohibits mobility and nucleation of surface melting.

The results of our MD simulations of laser-pulse irradiation of copper surfaces, where coupling between the ionic and electronic degrees of freedom was incorporated, provide significant insights pertaining to dynamics, energetics, and structure of surface superheating and melting processes. Furthermore, our observations of superheating and structural annealing of the (111) surface suggest further experiments as well as surface processing techniques.

This research is supported by the U.S. Department of Energy, Grant No. DE-FG05-86ER-45234. Partial support to H.H. from the Academy of Finland, assistance by R. N. Barnett, C. L. Cleveland, and W. D. Luedtke, and a useful correspondence with I. Koponen are gratefully acknowledged.

---

*Permanent address: Department of Physics, University of Jyväskylä, SF-40351 Jyväskylä, Finland.

[1] *Laser Annealing of Semiconductors*, edited by J. M. Poate and J. Mayer (Academic, New York, 1982); *Laser and Electron Beam Processing of Materials*, edited by C. W. White and P. S. Peercy (Academic, New York, 1980); M. Bass, *Laser Materials Processing* (North-Holland, Amsterdam, 1993).

[2] For an early molecular dynamics simulation of laser-annealing see C. L. Cleveland, U. Landman, and R. N. Barnett, Phys. Rev. Lett. **49**, 790 (1982).

[3] H. E. Elsayed-Ali *et al.*, Phys. Rev. Lett. **58**, 1212 (1987).

[4] (a) J. W. Herman and H. E. Elsayed-Ali, Phys. Rev. Lett. **68**, 2952 (1992); (b) **69**, 1228 (1992); (c) we have chosen copper surfaces for our simulations because of our previous extensive experience with this material.

[5] M. Faraday, Proc. R. Soc. London **10**, 440 (1860).

[6] See review by F. van der Veen, B. Pluis, and A. W. Denier van der Gon, in *Kinetics of Ordering at Surfaces*, edited by M. G. Lagally (Plenum, New York, 1990), p. 343.

[7] (a) P. Stoltze, J. K. Norskov, and U. Landman, Phys. Rev. Lett. **61**, 440 (1988); P. Stoltze, J. Chem. Phys. **92**, 6306 (1990); (b) H. Hakkinen and M. Manninen, Phys. Rev. B **46**, 1725 (1992); (c) E. T. Chen, R. N. Barnett, and U. Landman, Phys. Rev. B **40**, 924 (1989).

[8] R. N. Barnett and U. Landman, Phys. Rev. B **44**, 3226 (1991), and references therein.

[9] S. M. Foiles, Phys. Rev. B **32**, 3409 (1985).

[10] S. I. Anisimov, B. L. Kapeliovich, and T. L. Perelmann, Zh. Eksp. Teor. Fiz. **66**, 776 (1974) [Sov. Phys. JETP **39**, 375 (1974)], and discussion following Eq. (1) in it; for the theory of electron-phonon coupling, see M. I. Kaganov, I. M. Lifshitz, and L. V. Tanatarov, Zh. Eksp. Teor. Fiz. **31**, 232 (1957) [Sov Phys. JETP **4**, 173 (1957)].

[11] W. H. Press *et al.*, *Numerical Recipes* (Cambridge Univ. Press, New York, 1986).

[12] (a) A similar expression was used in the context of studies of energetic displacement cascades by M W. Finnis, P. Agnew, and A. J. E. Foreman, Phys. Rev. B **44**, 567 (1991); for other recent theoretical studies on the same subject see (b) I. Koponen and M. Hautala, Nucl. Instrum. Methods Phys. Res., Sect. B **69**, 182 (1992); (c) C. P. Flynn and R. S. Averback, Phys. Rev. B **38**, 7118 (1988); A. Caro and M. Victoria, Phys. Rev. A **40**, 2287 (1989).

[13] (a) *American Institute of Physics Handbook*, edited by D. E. Gray (McGraw-Hill, New York, 1972). (b) We note that in our simulations of laser irradiation of copper the peak intensities of the 4 ps laser pulses were $I_0=5\times10^9$ W/cm^2 and 8×10^9 W/cm^2, with the former resulting in superheating and the latter in melting of Cu(111). The superheating pulse corresponds to a total energy of 10^{-2} J/cm^2. In the experiments on superheating of Pb(111) laser pulses of the order of 200 ps with peak intensities of the order of 3.5×10^7 W/cm^2 were used [4(b)], corresponding to a total energy of 0.3×10^{-2} J/cm^2. The absorption length used in our simulation $\alpha^{-1}=20$ Å and in the experiment on Pb(111) (with wavelength $\lambda=1.16$ μm) $\alpha^{-1}=140$ Å. Taking into account the larger thermal conductivity of Cu than that of Pb [κ(Cu)$\sim5\kappa$(Pb)] we estimate that the lattice thermal effects of our pulses are comparable to experimentally realizable conditions.

[14] We note that in the time scale of our interest ($t<60$ ps), a "quasiequilibrium" state is reached, where T_e and T_l remain close to each other, with T_l somewhat higher than T_e, and both slowly equilibrating toward the bulk reference temperature $T_b=1100$ K.

[15] U. Landman and W. D. Luedtke, Appl. Surf. Sci. **60/61**, 1 (1992).

[16] H. Hakkinen, J. Merikoski, and M. Manninen, J. Phys. Condens. Matter **3**, 2755 (1991).

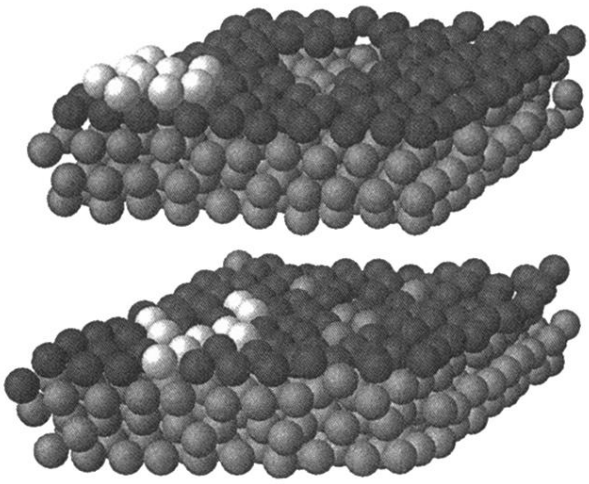

FIG. 4. Atomic configuration of a Cu(111) surface containing a vacancy cluster and an adlayer island (brightest atoms) prior to irradiation (top), and a configuration recorded 20 ps after the termination of a superheating laser pulse (bottom). Dark and grey spheres correspond to atoms in the topmost surface layer and in the layers below it. Note that in the annealed surface the atoms originating at the adlayer island did not migrate to fill the vacancy cluster.